JPET Fast Forward. Published on November 2, 2004 as DOI: 10.1124/jpet.104.077164

JPET77164

Poly(ADP-ribose) polymerase promotes cardiac remodeling, contractile failure and translocation of apoptosis-inducing factor in a murine experimental model of aortic banding and heart failure

[1]Chun-Yang Xiao, [1]Min Chen, [1]Zsuzsanna Zsengellér, [1]Hongshan Li, [2]Levente Kiss, [2]Márk Kollai, [1,2]Csaba Szabó

[1]Inotek Pharmaceuticals Corporation, Suite 419E, 100 Cummings Center, Beverly, MA 01915; USA

(CY X, MC, ZZ, HL, CS)

[2]Department of Human Physiology and Clinical Experimental Research, Semmelweis University, Budapest, Hungary

(LK, MK, CS)

JPET77164

Running title: PARP, AIF and chronic heart failure

*Author for correspondence:

Csaba Szabó, M.D., Ph.D.,

Inotek Pharmaceuticals Corporation, Suite 419E,

100 Cummings Center, Beverly, MA 01915, USA

Phone: (978) 232 9660 Fax: (978) 232 8975; E-mail: szabocsaba@aol.com

Number of text pages: 28

Number of tables: 1

Number of figures: 8

Number of references: 40

Number of words in abstract: 217

Number of words in introduction: 371

Number of words in discussion: 1486

Non-standard abbreviations: AIF: apoptosis-inducing factor; PARP: poly(ADP-ribose) polymerase

JPET Fast Forward. Published on November 2, 2004 as DOI: 10.1124/jpet.104.077164
This article has not been copyedited and formatted. The final version may differ from this version.

Abstract

Oxidant stress - induced activation ofpoly(ADP-ribose) polymerase (PARP) plays a role in the pathogenesis of various cardiovascular diseases. We have now investigated the role of PARP in the process of cardiac remodeling and heart failure in a mouse model of heart failure induced by transverse aortic constriction (banding). The catalytic activity of PARP was inhibited by the potent PARP inhibitor INO-1001 or by PARP-1 genetic deficiency. PARP inhibition prevented the pressure-overload induced decrease in cardiac contractile function, despite the pressure gradient between both carotid arteries being comparable in the two experimental groups. The development of hypertrophy, the formation of collagen in the hearts, and the mitochondrial-to nuclear translocation of the cell death factor AIF (apoptosis-inducing factor) were attenuated by PARP inhibition. The ability of the inhibitor to block the catalytic activity of PARP was confirmed by immuno-histochemical detection of poly(ADP-ribose), the product of the enzyme in the heart. Plasma levels of INO-1001, as measured at the end of the experiments, were in the concentration range sufficient to block the oxidant-mediated activation of PARP in murine cardiac myocytes *in vitro*. Myocardial hypertrophy and AIF translocation was also reduced in PARP-1 deficient mice undergoing aortic banding, when compared to their wild-type counterparts. Overall, the current results demonstrate the importance of poly(ADP-ribos)ylation in the pathogenesis of banding-induced heart failure.

JPET Fast Forward. Published on November 2, 2004 as DOI: 10.1124/jpet.104.077164
This article has not been copyedited and formatted. The final version may differ from this version.

Introduction

Poly(ADP-ribose) polymerase-1 (PARP-1), a monomeric enzyme present in eukaryotes, is the major isoform of an expanding family of poly(ADP-ribosyl)ating enzymes (overviewed in Virág and Szabó, 2002). The main isoform of the family, PARP-1, primarily functions as a DNA damage sensor in the nucleus. Upon binding to damaged DNA mainly through the second zinc finger domain, PARP-1 forms homodimers and catalyzes the cleavage of NAD^+ into nicotinamide and ADP-ribose and uses the latter to synthesize branched nucleic acid-like polymers poly(ADP-ribose) covalently attached to nuclear acceptor proteins. The biological role of PARP-1 is complex and includes the regulation of DNA repair and maintenance of genomic integrity.

PARP-1 has been implicated in a variety of pathophysiological processes. PARP is an energy-consuming enzyme, which transfers ADP ribose units to nuclear proteins. As a result of this process, the intracellular nicotinamide dinucleotide (oxidized) (NAD^+) and adenosine 5'-triphosphate (ATP) levels remarkably decrease, resulting in cell dysfunction and cell death via the necrotic route (overviewed in Virág and Szabó, 2002).

PARP becomes activated in response to DNA single-strand breaks, which can develop as a response to free radical and oxidant cell injury. Oxidative and nitrosative stress triggers the activation of the nuclear enzyme poly(ADP-ribose) polymerase (PARP), which contributes to the pathogenesis of various cardiovascular diseases including myocardial infarction and ischemia-reperfusion and heart failure (overviewed in Szabó et al., 2004). Recent studies have implicated the importance of mitochondrial

dysfunction and mitochondrial cell death factors, including AIF (apoptosis-inducing factor) (Cregan et al., 2002) in the process of oxidant-induced cell death, and the potential role of PARP in regulating these factors in various cell types including the myocardium (Yu et al., 2002; Xiao et al., 2004).

In the present study, using INO-1001, a potent PARP inhibitor (Khan et al., 2003; Chen et al., 2004; Murthy et al., 2003; Xiao et al., 2004), we have investigated the role of PARP in the development of myocardial failure and hypertrophy in a banding-induced chronic heart failure. We have also investigated the potential translocation of AIF in this model, and the role of PARP in regulating this process. Some of the key findings obtained with the PARP inhibitor were also confirmed by comparing wild-type and PARP-1 deficient mice undergoing aortic banding.

Methods

Animals

C57BL/6 mice were purchased from Charles River. $PARP^{-/-}$ and wild-type $PARP^{+/+}$ mice originally derived from Dr. ZQ Wang's laboratory (Wang et al., 1995) were maintained and bred in our animal facility as previously reported (Liaudet et al., 2001). Animals were housed in cages in a specific pathogen-free room and exposed to a cycle of 12 hours light/12 hours dark and had free access to water and food. An acclimation period of at least 1 week was provided before initiating the experimental protocol. The investigation conformed to the *Guide for the Care and Use of Laboratory*

Animals published by the National Institutes of Health, and was performed with approval of the local Animal Care and Use Committee.

Transverse aortic constriction

Transverse aortic constriction (TAC) was performed as previously described (Rockman et al., 1991). Briefly, male mice (7-9 weeks old) were anesthetized with a mixture of ketamine (65 mg/Kg) and xylazine (5 mg/Kg). The chest and neck were shaved, and mice were placed in a supine position under body temperature control, and a midline cervical incision was made to expose the trachea. Mice were orally intubated with a 20 gauge tubing and ventilated with a tidal volume of 0.2 ml at a rate of 110 strokes/minute using a rodent respirator (Model 683, Harvard). The chest was opened at the second intercostals space. The transverse aortic arch was ligated between the innominate artery and left common carotid artery with a 27 gauge needle using 7-0 silk suture with the aid of dissecting microscope, and then the needle was promptly removed to yield a constriction of 0.4 mm in diameter. The chest was closed in layers. The mice were kept on a heating pad until recovery from anesthesia. For the sham operation, the aorta was not ligated. Mice were studied at 9 weeks (pharmacological inhibitor studies) or 29 weeks (wild-type vs. PARP-1 knockout mice) after TAC.

Administration of INO-1001

The isoindolinone-based PARP inhibitor INO-1001 (Khan et al., 2003; Murthy et al., 2004) (30 mg/kg/day) or vehicle were administered orally (via drinking water) to aortic banded or sham-operated mice after surgical operation and continued to 9 weeks.

INO-1001 was dissolved into 5% dextrose injection USP (Abbott Labs) and diluted 100 times with water. The drug solution was changed every 2 days.

Measurement of cardiac function

To measure arterial pressure, 2 high-fidelity catheter tip transducers (1.4F, Millar) were used. One was inserted into the right carotid artery and advanced to the left ventricle for measurement of LV pressure and LV dP/dt. After measurement of LV function, the transducer was back to carotid artery. The another transducer was inserted into left carotid artery. The pressure in both carotid arteries was measured simultaneously and the pressure gradient between carotid arteries was calculated.

Additional measurements

At the conclusion of the studies, mice were scarified by an overdose of drug. Before the heart was isolated, the chest was opened to determine whether pleural effusion was present. The heart, lung and liver were removed and their weights were measured. Organ weights were normalized to body weight. In addition, in a separate set of studies C57BL/6 mice treated with INO-1001 and undergoing aortic banding (methods as above) were sacrificed at 1 and 9 weeks, plasma samples and myocardial tissues were obtained at 1 and 9 weeks of heart failure, and concentration of INO-1001 was measured by HPLC (N=5 animals/group).

In mice that died spontaneously, organs were also removed at autopsy. In these mice, the deaths were ascribed to heart failure, if pleural effusion had occurred, and then increased lung weight to body weight was confirmed.

Immunohistochemical analysis for PARP activation and AIF translocation

Immunohistochemical detection of poly(ADP-ribose) and apoptosis-inducing factor (AIF) was performed as previously described (Xiao et al., 2004). Primary antibodies used for the stainings were chicken polyclonal anti-poly(ADP-ribose) antibody (Tulip Biolabs) and rabbit polyclonal anti-AIF antibody (Chemicon).

Collagen staining

For collagen staining, fixed blocks of ventricular tissue was embedded in paraffin, and 5 μm-thick sections were cut from each block. The section was deparaffinized, rehydrated, and stained with Masson's trichrome using a staining kit (Sigma, HT15).

Preparation of mitochondrial, cytosolic, and nuclear fractions and Western blot analysis.

Fresh ventricles were cut into small pieces in ice-cold MSE buffer [in mmol/l: 225 mM mannitol, 75 mM sucrose, 1.0 mM EGTA, 20 mM HEPES (KOH), pH 7.4]. The samples were then resuspended in 3 volumes of MSE buffer supplemented with 1 mM dithiothreitol, and protease inhibitors (200 X cocktail solution, Sigma). Subcellular fractions were prepared as described, followed by Western blotting for AIF (Gottlieb et al., 1995; Chen et al., 2001). The heart was further homogenized for 5 s at power 3 output by a polytron homogenizer (PT1200 C; Kinematica, Switzerland). The homogenates were filtered through a 50 mesh screen to remove unbroken tissue, and then centrifuged at 600 × g at 4ºC for 10 min. The supernatant was centrifuged for 10 min at 8,000 × g. The

JPET Fast Forward. Published on November 2, 2004 as DOI: 10.1124/jpet.104.077164
This article has not been copyedited and formatted. The final version may differ from this version.

pellet obtained was used as mitochondrial fraction, and was washed twice and resuspended in MSE buffer. The 8,000 × *g* supernatant was re-centrifuged at 15,000 × *g* at 4ºC for 20 min, and the resulting supernatant was used as soluble cytosolic fraction.

To obtain nuclear extracts, the 600 × *g* nuclear pellet was washed twice with TMS buffer [in mmol/l: 240 sucrose, 10 Tris (pH 7.40), 1.5 $MgCl_2$] and incubated with 0.1% of Triton X-100 in TMS buffer for 15 min on ice. The nuclei were pelleted by centrifugation at 600 × *g* for 10 min and washed three times with 5 ml TMS buffer without Triton X-100. The final pellet of nuclei was resuspended 1/1 (v/v) in extract buffer [in mmol/l: 400 NaCl, 20 Tris (pH 7.5), 1.5 $MgCl_2$, 1 DTT, 25% glycerol], and incubated at 4ºC with gentle shaking for 1 hr. The nuclei were pelleted again at 600 × *g* for 10 min, and the resulted supernatant was further centrifuged at 15,000 × *g* for 20 min to obtain nuclear extract.

Samples containing 30 μg protein were subjected to electrophoresis on polyacrylamide gels (Invitrogen) and then transferred to nitrocellulose membrane. After blocking in 3% nonfat milk and 0.05% Tween 20 in phosphate-buffered saline, blot were incubated with antibody to AIF (murine polyclonal, Chemicon. Inc).

In vitro myocyte isolation and PARP inhibition studies

Isolation of ventricular myocytes from mice was conducted as described (Chen et al., 2004). Hearts were excised and mounted in a Langendorff perfusion apparatus and perfused for ~5 min with Ca-free Krebs-Henseleit bicarbonate (KHB) buffer containing (in mM) 120 NaCl, 5.4 KCl, 1.2 $MgSO_4$, 1.2 NaH_2PO_4, 5.6 glucose, 20 $NaHCO_3$, 10 2,3-butanedione monoxime (BDM; Sigma), and 5 taurine (Sigma), gassed with 95% O_2-5%

CO_2, followed by a 15-20 min perfusion with same KRB buffer containing 25 μM $CaCl_2$, 0.1% collagenase (Worthington Biochemical Corp., Freehold, NJ) and 0.1% BSA. Thereafter, ventricular tissue was chopped and incubated for 10 min in the same medium supplemented with 1% BSA. The ventricular tissue was then dispersed and filtered. The resultant myocytes were washed twice with fresh KRB buffer containing 1% BSA and 25 μM $CaCl_2$, and then the Ca^{2+} concentration was increased to 1.0 mM gradually. Finally, the myocyte pellets were washed and suspended in MEM medium containing 1.2 mM Ca^{2+} (Sigma, M1080). Myocytes were plated in laminin-precoated plates or glass coverslips at a density of 10^5 cells/cm^2. After 1 hr plating in MEM medium with 5% fetal calf serum, the medium was changed to FBS-free MEM. Following overnight culture, myocytes were subjected to H_2O_2 treatment at 200 μM in the presence or absence of various concentrations of INO-1001. Activation of PARP was measured by incorporation of radiolabeled NAD^+ as previously described (Garcia Soriano et al., 2001).

Statistical Analysis

Results are expressed as mean ± SEM. Differences between means were evaluated by unpaired 2-tailed Student's *t* test.

JPET Fast Forward. Published on November 2, 2004 as DOI: 10.1124/jpet.104.077164
This article has not been copyedited and formatted. The final version may differ from this version.

Results

Effect of INO-1001 on hemodynamics

To examine the effect of INO-1001 on hemodynamic loading conditions of aortic banded mice, we measured the mechanical function. Table 1 summarizes the hemodynamic results. At 9 weeks after banding, LVSP increased significantly in banded mice compared to sham-operated mice. Hearts from vehicle-treated banded mice showed a 22% and 14% reduction in maximal dP/dt (+dP/dt) and minimal dP/dt (-dP/dt) compared with those from sham-operated mice, indicating pressure-overload impaired cardiac function. Treatment with INO-1001 prevented the pressure-overload induced decrease in contractile function despite the pressure gradient between both carotid arteries was comparable in the vehicle-treated banded group (51.2 ± 5.1 mmHg) versus the INO-1001 treatment banded group (50.2 ± 9.5 mmHg).

Effect of INO-1001 on the load-induced increase in heart weight and mortality

To examine whether INO-1001 attenuates load-induced cardiac hypertrophy, we treated aortic banded mice with INO-1001 or vehicle for 9 weeks after surgery. Aortic banded mice had a significant increase in heart weight at end of experiment compared with sham-operated mice. Heart weight or LV weight to tibial length (HW/TL, LV/TL) ratio increased by 100.5% or 117.9% in the vehicle-treated banded mice. Importantly, however, in INO-1001 treatment banded mice, HW/TL or LV/TL ratio rose by 39.0% or 60.9%, which was significantly lower than in the vehicle-treated banded mice (Figure 1).

The body weights and tibial lengths were not different among these groups. Furthermore, 9 weeks after TAC, aortic banded mice exhibited increased lung weight (Table 1), indicating the development of pulmonary congestion. In contrast, INO-1001 treated banded mice showed a significant decrease in lung weight.

The all-cause mortality rate of TAC was not different for vehicle-treated banded mice and INO-1001 treated banded mice (Figure 2). All sham-operated mice survived to the time of experiment. 45 mice of 72 in the vehicle-treated banded group and 32 mice of 61 in the INO-1001 treatment mice died prematurely. 21 mice in vehicle-treated banded mice (29.2%) and 11 mice in the INO-1001 treatment banded mice (18.1%) died of heart failure, judged by postmortem findings. These mice had massive pleural effusion and severe lung congestion (lung wet weight 400.1 ± 29.6 mg, range 189-782 mg). All mice developed severe hypertrophy (heart weight 216 ± 12.7 mg, range 135-451.8 mg).

There was a massive staining of collagen in the myocardium of banded mice, which was markedly reduced in the INO-1001 treated group of banded animals (Fig. 3).

The concentration of INO-1001 in plasma at 9 weeks after treatment in aortic banded mice was 1.24 ± 0.96 μM (n=4). However, at 1 week after the start of the experiment, plasma PARP inhibitor levels amounted to only 0.27±0.12 μM, indicating a gradual build-up of plasma INO-1001 concentrations in the animals subjected to its administration in the drinking water. Similarly, INO-1001 levels in the heart only amounted to 0.18±0.09 μM at 1 week, whereas they increased to 0.41±0.12 μM at 9 weeks. *In vitro* pretreatment with 1 μM INO-1001 fully prevented PARP activation in cardiac myocytes challenged with hydrogen peroxide (n=4). At a 10-times lower

concentration (0.1 μM INO-1001), PARP activation in hydrogen peroxide challenged myocytes was reduced by 56±7% ($p<0.05$, n=4).

Effect of INO-1001 on the load-induced PARP activation and AIF translocation

To examine whether PARP was activated in the myocardium in response to chronic pressure overload, mice were killed 1, 4 and 9 weeks after the operation. Pressure overload caused increase in PARP activity, which reached its peak at 1 week, in both vehicle-treated and INO-1001 treated banded mice hearts compared with sham-operated mice heart. PARP activation in INO-1001 treated banded mice hearts was reduced and was similar to baseline level from 4 weeks after treatment (Fig 4).

PARP activation signals AIF release from mitochondria, resulting in a caspase-independent pathway of cell death (Yu et al., 2002; Xiao et al., 2004). We used immunohistochemical method to confirm AIF translocation in myocardial tissue. As shown in Figure 5, pressure overload induced AIF translocation. This phenomenon was also conforirmed by subcellular fractionation, followed by AIF Western blotting (Fig. 6). Similar to the results of PARP activation, the peak of AIF translocation occurred at 1 week after aortic banding and then decreased in both groups. INO-1001 prevented AIF translocation from 4 weeks after operation (Fig 5).

Studies in wild-type and PARP-1 deficient animals

In order to further characterize the involvement of PARP in heart failure, $PARP^{-/-}$ and wildtype littermate mice ($PARP^{+/+}$) were subjected to long-term aortic banding. After 29 weeks, both $PARP^{-/-}$ and $PARP^{+/+}$ mice displayed increased contractile function

in response to pressure overload (data not shown). Aortic banding caused a significant myocardial hypertrophy in $PARP^{+/+}$ mice compared with sham-operated mice (Fig. 7). The percentage of increase HW/TL and LVW/TL was 49.4% and 59.9%, respectively. The increased percentage of HW/TL and LVW/TL in $PARP^{-/-}$ mice was 23.2% and 29.5%,, which was significantly ($p<0.05$) lower than in the $PARP^{+/+}$ mice. The pressure gradient was comparable in both $PARP^{-/-}$ and $PARP^{+/+}$ banded mice (96.0 ± 28.8 mmHg vs. 99.4 ± 20.5 mmHg, n=4 in each group). These results demonstrate that $PARP^{-/-}$ mice develop less hypertrophy compared with $PARP^{+/+}$ mice. AIF translocation from the mitochondrial to nuclear fraction was noted in the wild-type mice subjected to aortic banding, but not in the $PARP^{-/-}$ banded mice (Fig. 8). However, the extent of these changes at 29 weeks was less pronounced at 29 weeks than at 9 weeks, perhaps indicating that by 29 weeks of banding the peak of the AIF translocation has passed.

Discussion

The current study shows that aortic banding in mice induces chronic heart failure (CHF), evidenced by depression of left ventricular function and hypertrophy and collagenization of the heart. These results are consistent with earlier reports using similar experimental models. The impaired cardiac function is associated with a diffuse activation of PARP in the myocardium. The ability of INO-1001 to inhibit PARP in the cardiac myocytes was confirmed via immunohistochemical detection of poly(ADP-ribose) activation. In addition, plasma and myocardial concentrations of the PARP inhibitor were found sufficient to block oxidant-induced PARP activation in cardiac

myocytes *in vitro*. Direct functional measurements demonstrate the maintenance of cardiac output in the PARP inhibitor treated animals undergoing aortic banding.

Reactive oxygen species (superoxide, hydrogen peroxide, hydroxyl radical) are overproduced in the failing myocardium (Ekelund et al., 1999; Mihm et al., 2001). There is also an overproduction of nitric oxide, due to the expression of the inducible isoform of NO synthase (iNOS) (Fukuchi et al., 1998; Vejlstrup et al., 1998). Importantly, a recent study has suggested correlation between chronic overexpression of iNOS and peroxynitrite generation with cardiac enlargement, conduction defects, sudden cardiac death, and, less commonly, heart failure in mice (Mungrue et al., 2002). In the present, banding-induced CHF model, evidence was also found for upregulation of the endothelial isoform of NOS (Dai et al., 2004). The combination of NO and superoxide yields peroxynitrite, which is able to trigger DNA single strand breakage and activation of PARP (overviewed in Virág and Szabó, 2002). Peroxynitrite generation has been demonstrated in various models of CHF, including the current model of banding (Bouloumie et al., 1997), and this species has been shown to impair cardiac function via multiple mechanisms (Mihm et al., 2001; Pacher et al., 2003). The increased sensitivity of the myocytes to the toxic effects of NO has been directly demonstrated in a banding-induced cardiac hypertrophy model (Brookes et al., 2001).

A recently characterized mechanism of myocardial dysfunction involves the activation of the nuclear enzyme PARP by DNA single strand breaks generated in response to increased oxidative and nitrosative stress. Evidence for the importance of this pathway has been demonstrated in hearts subjected to regional or global ischemia and reperfusion (overviewed in Szabó et al., 2004). The mode of PARP inhibitors'

cardioprotective action involves a conservation of myocardial energetics, as well as a prevention of the up-regulation of various pro-inflammatory pathways (cytokines, adhesion receptors, mononuclear cell infiltration) triggered by ischemia and reperfusion (overviewed in Virág and Szabó, 2002). It is conceivable that PARP inhibition exerts beneficial effects in the current model by affecting both above referenced pathways of injury, and also by suppressing positive feedback cycles initiated by them. It is more likely that the reduction in myocardial hypertrophy by INO-1001 (which is thought to be mediated by the up-regulation of growth factors) is mediated by the PARP-mediated modulation of signal transduction and gene expression pathways. Indeed, recent studies implicate the ability of PARP to regulate the expression of growth factors *in vitro* (Obrosova et al., 2004).

Multiple reports indicate the importance of PARP activation in the development of mitochondrial dysfunction under conditions of oxidative stress (Yu et al., 2002; Du et al., 2003). Even though the major isoform of the PARP family, PARP-1, is widely considered as a nuclear enzyme, there may also be a mitochondrial isoform (Du et al., 2003), and there is a nuclear-to mitochondrial signaling process, which initiates early mitochondrial alterations, as demonstrated in thymocytes (Virág et al., 1998), in neurons (Yu et al., 2002; Komjáti et al., 2004), in cardiac myocytes *in vitro* (Chen et al., 2004) and in myocardial infarction *in vivo* (Xiao et al., 2004). The current findings, demonstrating that PARP inhibition with INO-1001 or genetic PARP-1 deficiency reverse mitochondrial-to nuclear translocation of AIF in CHF, are consistent with prior studies demonstrating that PARP-1 regulates the translocation of this cell death factor.

It is interesting to note that PARP inhibitor prevented PAR accumulation at 4 or 9 weeks after the banding, but this inhibitory effect is not obvious at 1 week. The same pattern was seen in Figure 5, where the inhibition of AIF translocation by INO-1001 was less effective at 1 week than at 4 or 9 weeks later. Considering the gradual increase in plasma and myocardial INO-1001 levels seen in the present study, it is conceivable that myocardial INO-1001 levels at 1 week did not yet reach sufficient concentrations at the beginning of the study to provide full inhibition of PARP. Additional studies, with delayed administration of the PARP inhibitor are needed to determine the therapeutic window of opportunity, and to evaluate whether delayed treatment with PARP inhibitors is able to arrest cardiac hypertrophy or restore myocardial function in CHF.

Prior studies have demonstrated the importance of apoptosis, caspases (e.g. Hayakawa et al., 2003; Chandrashekhar et al., 2004), and a variety of cellular pathways, including protein kinase C (PKC) activation (e.g. Takeishi et al., 1998; Koide et al., 2003) in the pathogenesis of CHF. There are also many studies demonstrating TUNEL positivity in a small (approximately 0.3%) population of cells in murine CHF models (Jiang et al., 2004). In human samples, the percentage of TUNEL positivity can be higher (up to 2%) (Di Napoli et al., 2003; Hughes, 2003). What, then, is the relationship between PARP activation, AIF translocation, and the previously described pathways of apoptosis and CHF? First of all, we would like to emphasize, that, although AIF is termed "apoptosis-inducing" factor, its role goes beyond apoptosis, and it plays a role in a variety of cell death processes (necrotic, oxidant stress induced, and mixed type) (Cregan et al., 2004; Hong et al., 2004). Thus, AIF translocation per se should not be viewed as a hallmark or marker of apoptosis. Indeed, the very small percentage of TUNEL positive

myocytes seen in CHF myocardium (which has also been observed in the current model; unpublished data), is consistent with this view. AIF translocation can lead to DNA fragmentation, which, however, is caspase-independent. Therefore, its pattern is different from the typical, caspase-mediated DNA cleavage pattern, and may not be detectable by conventional TUNEL assays. Furthermore, it is not yet entirely clear whether AIF translocation in CHF is a sufficient, or merely a necessary factor for its ability to induce its hallmark large-scale chromatin condensation.

We also need to distinguish between PARP cleavage (a marker, but not necessarily an executor of apoptosis) and PARP activation (induced by DNA strand breaks). The latter process can only occur when PARP is uncleaved, as cleaved PARP is catalytically inactive (overviewed in Duriez and Shah, 1997; Virág and Szabó, 2002). The fact that we see widespread poly(ADP-ribose) accumulation in the CHF myocardium indicates that some (possibly most of the) PARP remains in the uncleaved, and functionally active state. In fact, a recent report finds no evidence for PARP cleavage in murine or human hearts with CHF (Pillai et al., 2004). The protection against CHF reported by caspase inhibitors, therefore, is most likely related to a pathway that is parallel and independent from the pathway governed by PARP activation.

As far as potential connections between PKC and PARP go, recent work, conducted using an *in vitro* model of diabetic complications (endothelial cells placed in high glucose), demonstrates that protein kinase C activation is governed by GAPDH, and in that experimental system PARP inhibitors indirectly inhibit PKC activation, by preventing GAPDH poly(ADP-ribosyl)ation (Du et al., 2003). At this point, it is unknown whether PARP/PKC interactions are also present in CHF.

In a prior model of CHF induced by chronic coronary artery ligation, the phenanthridinone-based PARP inhibitor PJ34 was found to attenuate myocardial hypertrophy, and improved the endothelial function of blood vessels (Pacher et al., 2002). The current study extends these findings. The novel aspects of the current work include direct demonstration that PARP inhibition improves cardiac output, attenuates cardiac fibrosis, and tends to reduce CHF-related mortality in a model of banding-induced CHF. The current report is also the first one to demonstrate the phenomenon of mitochondrial-to-nuclear translocation of AIF in CHF, and implicates the regulatory role of PARP in this process. While the present work was in review, a recent study appeared (Pillai et al., 2004) demonstrating an over-expression of PARP-1 enzyme in murine and human CHF models. Thus, the increased poly(ADP-ribose) staining seen in our studies may be a combined consequence of PARP activation and PARP upregulation. The Pillai et al. report also shows, that (similar to our results), PARP-1 deficient mice are protected against the hypertrophy response induced by aortic banding. Overall, our studies (Pacher et al., 2002 and the current study) as well as other recent studies (Pillai et al., 2004) support the view that PARP activation importantly contributes to the pathogenesis of cardiovascular dysfunction in experimental models of CHF, and strengthens the notion that PARP inhibition may represent a novel approach for the experimental therapy of CHF.

References

Bouloumie A, Bauersachs J, Linz W, Scholkens BA, Wiemer G, Fleming I, Busse R (1997) Endothelial dysfunction coincides with an enhanced nitric oxide synthase expression and superoxide anion production. *Hypertension* 30:934-941.

Brookes PS, Zhang J, Dai L, Zhou F, Parks DA, Darley-Usmar VM, Anderson PG (2001)Increased sensitivity of mitochondrial respiration to inhibition by nitric oxide in cardiac hypertrophy. *J Mol Cell Cardiol* 33:69-82.

Chen M, He H, Zhan S, Krajewski S, Reed JC, Gottlieb RA (2001) Bid is cleaved by calpain to an active fragment in vitro and during myocardial ischemia/reperfusion. *J Biol Chem* 276:30724-30728.

Chandrashekhar Y, Sen S, Anway R, Shuros A, Anand I (2004) Long-term caspase inhibition ameliorates apoptosis, reduces myocardial troponin-I cleavage, protects left ventricular function, and attenuates remodeling in rats with myocardial infarction. *J Am Coll Cardiol* 43:295-301

Chen M, Zsengeller Z, Xiao CY, Szabó C (2004) Mitochondrial-to-nuclear translocation of apoptosis-inducing factor in cardiac myocytes during oxidant stress: potential role of poly(ADP-ribose) polymerase-1. *Cardiovasc Res* 63:682-688.

Cregan SP, Dawson VL, Slack RS (2004) Role of AIF in caspase-dependent and caspase-independent cell death. *Oncogene* 23:2785-2796.

Cregan SP, Fortin A, MacLaurin JG, Callaghan SM, Cecconi F, Yu SW, Dawson TM, Dawson VL, Park DS, Kroemer G, Slack RS (2002) Apoptosis-inducing factor is

involved in the regulation of caspase-independent neuronal cell death. *J Cell Biol* 158:507-517.

Dai ZK, Tan MS, Chai CY, Yeh JL, Chou SH, Chiu CC, Jeng AY, Chen IJ, Wu JR (2004) Upregulation of endothelial nitric oxide synthase and endothelin-1 in pulmonary hypertension secondary to heart failure in aorta-banded rats. *Pediatr Pulmonol* 37:249-256.

Di Napoli P, Taccardi AA, Grilli A, Felaco M, Balbone A, Angelucci D, Gallina S, Calafiore AM, De Caterina R, Barsotti A (2003) Left ventricular wall stress as a direct correlate of cardiomyocyte apoptosis in patients with severe dilated cardiomyopathy. *Am Heart J* 146:1105-1111.

Du L, Zhang X, Han YY, Burke NA, Kochanek PM, Watkins SC, Graham SH, Carcillo JA, Szabo C, Clark RS (2003) Intra-mitochondrial poly(ADP-ribosylation) contributes to NAD+ depletion and cell death induced by oxidative stress. *J Biol Chem* 278:18426-18433.

Du X, Matsumura T, Edelstein D, Rossetti L, Zsengeller Z, Szabo C, Brownlee M (2003) Inhibition of GAPDH activity by poly(ADP-ribose) polymerase activates three major pathways of hyperglycemic damage in endothelial cells. *J Clin Invest* 112:1049-1057

Duriez PJ, Shah GM (1997) Cleavage of poly(ADP-ribose) polymerase: a sensitive parameter to study cell death. *Biochem Cell Biol* 75:337-349.

Ekelund UE, Harrison RW, Shokek O (1999) Intravenous allopurinol decreases myocardial oxygen consumption and increases mechanical efficiency in dogs with pacing-induced heart failure. *Circ Res* 85:437-445.

Fukuchi M, Hussain SN, Giaid A (1998) Heterogeneous expression and activity of endothelial and inducible nitric oxide synthases in end-stage human heart failure: their relation to lesion site and beta-adrenergic receptor therapy. *Circulation* 98:132-139.

Gottlieb RA, Giesing HA, Engler RL, Babior BM (1995) The acid deoxyribonuclease of neutrophils: a possible participant in apoptosis-associated genome destruction. *Blood* 86:2414-2418.

Hayakawa Y, Chandra M, Miao W, Shirani J, Brown JH, Dorn GW 2nd, Armstrong RC, Kitsis RN (2003) Inhibition of cardiac myocyte apoptosis improves cardiac function and abolishes mortality in the peripartum cardiomyopathy of Galpha(q) transgenic mice. *Circulation* 108:3036-3041.

Hong SJ, Dawson TM, Dawson VL (2004) Nuclear and mitochondrial conversations in cell death: PARP-1 and AIF signaling. *Trends Pharmacol Sci* 25:259-264.

Hughes SE (2003) Detection of apoptosis using in situ markers for DNA strand breaks in the failing human heart. Fact or epiphenomenon? *J Pathol* 2003 201:181-186.

Jiang L, Huang Y, Hunyor S, dos Remedios CG (2003) Cardiomyocyte apoptosis is associated with increased wall stress in chronic failing left ventricle. *Eur Heart J* 24: 742-751.

Khan TA, Ruel M, Bianchi C, Voisine P, Komjati K, Szabo C, Sellke FW (2003) Poly(ADP-ribose) polymerase inhibition improves postischemic myocardial function after cardioplegia-cardiopulmonary bypass. *J Am Coll Surg* 197:270-277.

Koide Y, Tamura K, Suzuki A, Kitamura K, Yokoyama K, Hashimoto T, Hirawa N, Kihara M, Ohno S, Umemura S (2003) Differential induction of protein kinase C

isoforms at the cardiac hypertrophy stage and congestive heart failure stage in Dahl salt-sensitive rats. *Hypertens Res* 26:421-426.

Komjáti K, Mabley JG, Virág L, Southan GJ, Salzman AL, Szabó C (2004). Poly(ADP-ribose) polymerase inhibition protects neurons and the white matter and regulates the translocation of apoptosis-inducing factor in stroke. *Int J Mol Med,* 13: 373-382.

Liaudet L, Soriano FG, Szabo E, Virag L, Mabley JG, Salzman AL, Szabo C (2000) Protection against hemorrhagic shock in mice genetically deficient in poly(ADP-ribose)polymerase. *Proc Natl Acad Sci U S A* 97:10203-10208.

Mihm MJ, Coyle CM, Schanbacher BL, Weinstein DM, Bauer JA (2001) Peroxynitrite induced nitration and inactivation of myofibrillar creatine kinase in experimental heart failure. *Cardiovasc Res* 49:798-807.

Mungrue IN, Gros R, You X (2002) Cardiomyocyte overexpression of iNOS in mice results in peroxynitrite generation, heart block, and sudden death. *J Clin Invest* 109:735-743.

Murthy KGK, Xiao CY, Mabley JG, Chen M, Szabó C (2004) Activation of poly(ADP-ribose) polymerase in circulating leukocytes during myocardial infarction. *Shock* 21:230-234.

Obrosova IG, Minchenko AG, Frank RN, Seigel GM, Zsengeller Z, Pacher P, Stevens MJ, Szabó C (2004) Poly(ADP-ribose) polymerase inhibitors counteract diabetes- and hypoxia-induced retinal vascular endothelial growth factor overexpression. *Int J Mol Med*. 14:55-64.

Pacher P, Liaudet L, Bai P, Mabley JG, Kaminski PM, Virag L, Deb A, Szabo E, Ungvari Z, Wolin MS, Groves JT, Szabó C (2003) Potent metalloporphyrin peroxynitrite

decomposition catalyst protects against the development of doxorubicin-induced cardiac dysfunction. *Circulation* 107:896-904.

Pacher P, Liaudet L, Mabley J, Komjati K, Szabó C (2002) Pharmacologic inhibition of poly(adenosine diphosphate-ribose) polymerase may represent a novel therapeutic approach in chronic heart failure. *J Am Coll Cardiol* 40:1006-1016.

Pillai JB, Russell HM, Raman JS, Jeevanandam V, Gupta MP (2004) Increased expression of poly (ADP) ribose polymerase-1 contributes to caspase-independent myocyte cell death during heart failure. *Am J Physiol Heart Circ Physiol*. Sep 16 [Epub ahead of print]

Rockman HA, Ross RS, Harris AN, Knowlton KU, Steinhelper ME, Field LJ, Ross J Jr, Chien KR (1991) Segregation of atrial-specific and inducible expression of an atrial natriuretic factor transgene in an in vivo murine model of cardiac hypertrophy. *Proc Natl Acad Sci U S A* 88: 8277-8281.

Soriano FG, Virag L, Jagtap P, Szabo E, Mabley JG, Liaudet L, Marton A, Hoyt DG, Murthy KG, Salzman AL, Southan GJ, Szabó C (2001) Diabetic endothelial dysfunction: the role of poly (ADP-ribose) polymerase activation. *Nature Medicine* 7:108-113.

Szabó G, Liaudet L, Hagl S, Szabó C (2004) Poly(ADP-ribose) polymerase activation in the reperfused myocardium. *Cardiovasc Res* 61:471-480.

Takeishi Y, Chu G, Kirkpatrick DM, Li Z, Wakasaki H, Kranias EG, King GL, Walsh RA (1998) In vivo phosphorylation of cardiac troponin I by protein kinase Cbeta2 decreases cardiomyocyte calcium responsiveness and contractility in transgenic mouse hearts. *J Clin Invest* 102: 72-78.

Vejlstrup NG, Bouloumie A, Boesgaard S (1998) Inducible nitric oxide synthase (iNOS) in the human heart: expression and localization in congestive heart failure. *J Mol Cell Cardiol* 30:1215-1223.

Virág L, Salzman AL, Szabó C (1998): Poly (ADP-ribose) synthetase activation mediates mitochondrial injury during oxidant-induced cell death. *J Immunol* 161: 3753-3759.

Virag L, Szabó C (2002) The therapeutic potential of poly(ADP-ribose) polymerase inhibitors. *Pharmacol Rev*. 54:375-429.

Wang ZQ, Auer B, Stingl L, Berghammer H, Haidacher D, Schweiger M, Wagner EF (1995) Mice lacking ADPRT and poly(ADP-ribosyl)ation develop normally but are susceptible to skin disease. *Genes Dev* 9: 509-520.

Xiao CY, Chen M, Zsengeller Z, Szabó C (2004) Poly(ADP-ribose) polymerase contributes to the development of myocardial infarction in diabetic rats and regulates the nuclear translocation of apoptosis-inducing factor. *J Pharmacol Exp Ther* 310:498-504.

Yu SW, Wang H, Poitras MF, Coombs C, Bowers WJ, Federoff HJ, Poirier GG, Dawson TM, Dawson VL (2002) Mediation of poly(ADP-ribose) polymerase-1-dependent cell death by apoptosis-inducing factor. *Science* 297:259-263.

Footnotes section:

This work was supported by a grant from the National Institutes of Health: R01 HL59266 (to CS).

JPET Fast Forward. Published on November 2, 2004 as DOI: 10.1124/jpet.104.077164
This article has not been copyedited and formatted. The final version may differ from this version.

Legends for Figures

Figure 1. Reduced hypertrophic response to pressure-overload in mice subjected to aortic banding in the presence of the PARP inhibitor INO-1001. (A) Representative photographs of heart from vehicle-treated banded, INO-1001-treated banded and respective sham-operated mice 9 weeks after TAC. (B) The heart weight/body weight and LV weight/tibial length ratio were determined 9 weeks after TAC or sham operation. The error bars represent the SEM. *P<0.05 vs respective sham-operative mice. †P<0.05 INO-1001 treated *vs* vehicle-treated banded mice.

Figure 2. Survival of mice subjected to aortic banding in the presence and absence of the PARP inhibitor INO-1001. Curves showing premature deaths by heart failure and death by other causes from vehicle-treated banded, INO-1001-treated banded and sham-operated mice.

Figure 3. Effect of INO-1001 on collagen accumulation in aortic banded mouse hearts. Aortic banded and sham-operated mice were killed 9 weeks after operation. Treatment with INO-1001 after 4 weeks markedly reduced the accumulation of collagen in aortic banded mouse heart. Representative sections from 4-5 animals per group are shown. Bottom panels represent 4X higher magnification compared to the top panels.

Figure 4. Effect of INO-1001 on PARP activation in aortic banded mouse hearts. Aortic banded and sham-operated mice were killed 1, 4, 9 weeks after operation. PARP activation was detected by immunohistochemical staining as described under method. Treatment with INO-1001 after 4 weeks markedly reduced PARP activation in aortic banded mouse heart. Representative sections from 4-5 animals per group are shown.

Figure 5. Effect of INO-1001 on AIF translocation in aortic banded mouse hearts. Aortic banded and sham-operated mice were killed 1, 4, 9 weeks after operation. AIF translocation was detected by immunohistochemical staining as described under method. Treatment with INO-1001 after 4 weeks markedly reduced AIF translocation in aortic banded mouse heart.

Figure 6. Evidence for myocardial AIF translocation in CHF. Aortic banded and sham-operated mice were killed at 9 weeks after operation. AIF levels in cytosolic, mitochondrial and nuclear fractions were detected by Western blotting.

Figure 7. Effects of long term pressure-overload in PARP$^{-/-}$ mouse hearts. Heart weight to tibia length ratio in PARP$^{-/-}$ and PARP$^{+/+}$ mice were determined at 29 weeks after TAC. The error bars represent the SEM. *P<0.05 *vs.* respective sham-operative mice. †P<0.05 *vs.* PARP$^{+/+}$ mice.

Figure 8. AIF translocation in hearts of wild-type and PARP-1 deficient mice at 29 weeks of CHF. Aortic banded wild-type and PARP-1 deficient mice were killed at 29 weeks after operation. AIF levels in mitochondrial and nuclear fractions were detected by Western blotting. In wild-type mice there was evidence for loss of AIF in mitochondrial fractions, and an increase in nuclear fractions. Similar changes were not seen in the PARP-1 deficient hurts undergoing CHF.

JPET Fast Forward. Published on November 2, 2004 as DOI: 10.1124/jpet.104.077164
This article has not been copyedited and formatted. The final version may differ from this version.

Table 1. Improvement in cardiac function by PARP inhibition in chronic heart failure induced by aortic banding. Hemodynamic measurement and organ weight of 9-week aortic-banded mice treated with vehicle or INO-1001. Results are presented as mean ± SEM. *P<0.05 *vs* respective sham-operated group, †P<0.05 INO-1001 treated banded group *vs* vehicle-treated banded group.

	Vehicle		INO-1001	
	Sham	Banded	Sham	Banded
		(n=9-17)	(n=7-12) (n=5-8)	(n=10-16)
Body weight, g	31.2±0.9	29.8±0.8	33.1±0.6	31.8±0.6
Lung weight, mg	184.1±7.8	289.8±41.3*	175.8±4.6	206.4±16†
Liver weight, g	1.29±0.05	1.30±0.04	1.33±0.08	1.30±0.03
Lung weight/body weight, mg/g	5.9±0.3	10.3±1.8*	5.3±0.2	6.5±0.5†
Aortic pressure gradient, mmHg	3.1±1.4	51.2±5.0*	2.8±0.7	50.2±9.5*
Heart rate, bpm	352±36	323±21	322±24	326±31
LVSP, mmHg	126.5±3.0	152.4±6.9*	123.8±7.9	169.9±7.5*
dP/dt, mmHg/mS	5.78±0.24	4.51±0.21*	5.53±0.30	5.48±0.24†
-dP/dt, mmHg/mS	5.47±0.20	4.71±0.32*	5.69±0.23	6.13±0.34†

Results are presented as mean ± SEM. *P<0.05 *vs* respective sham-operated group, †P<0.05 *vs* vehicle-treated banded group.

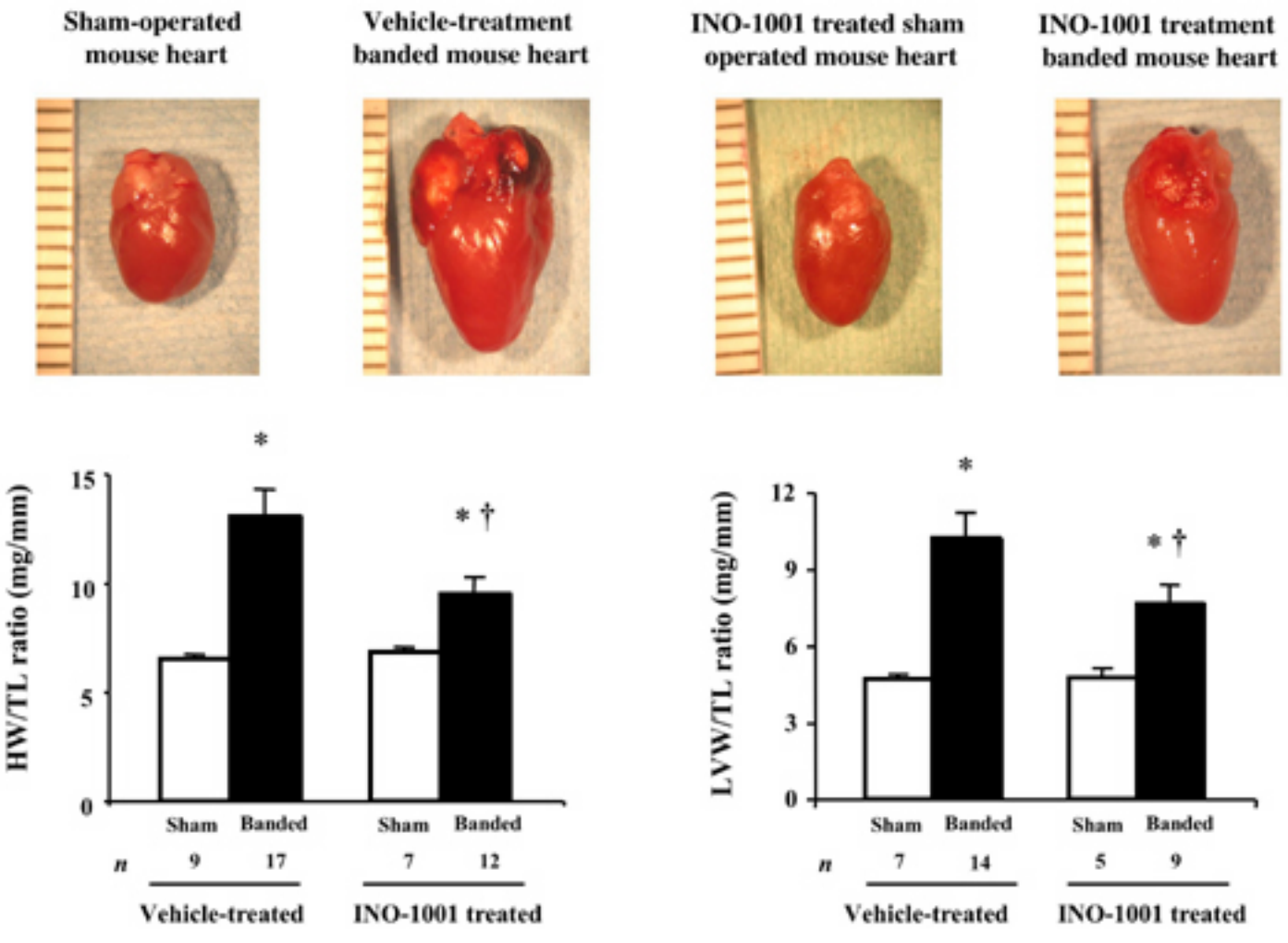

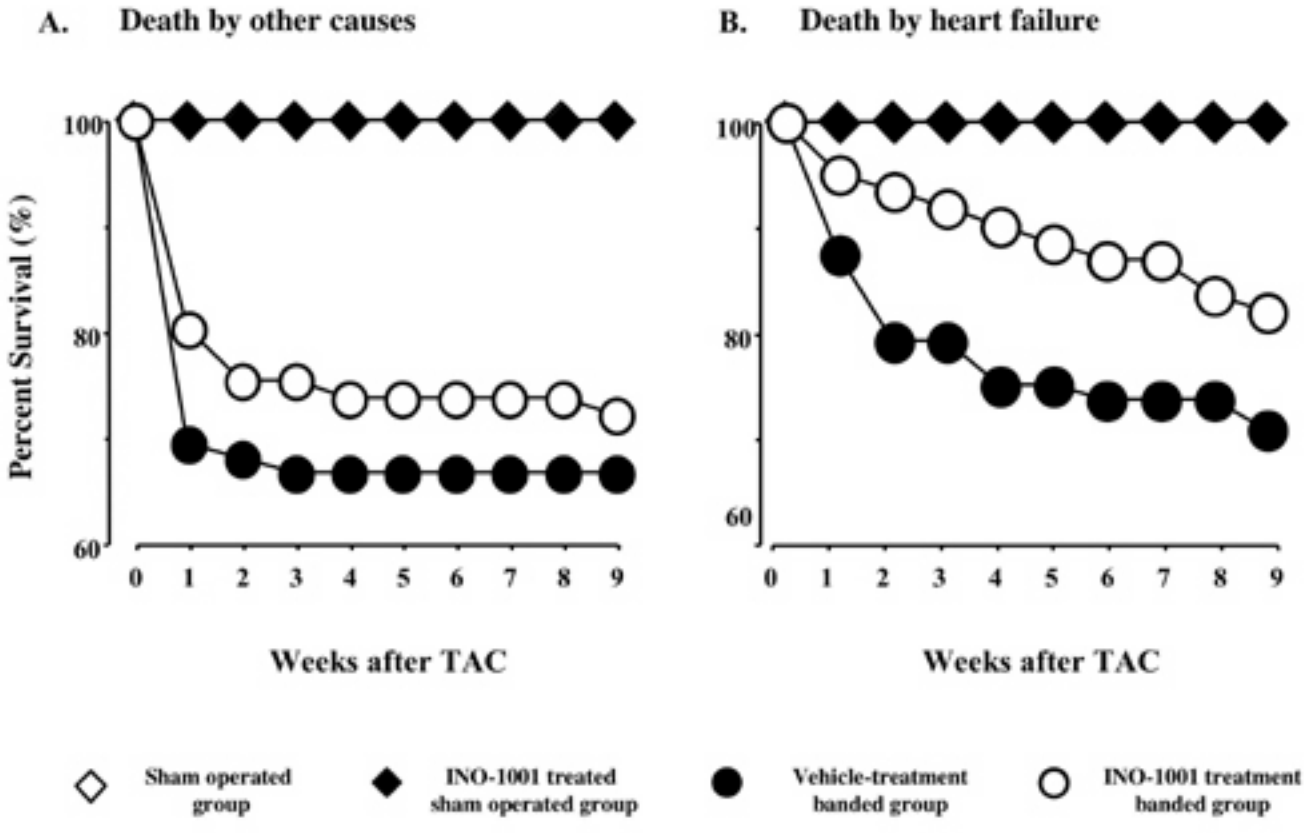

Figure 2

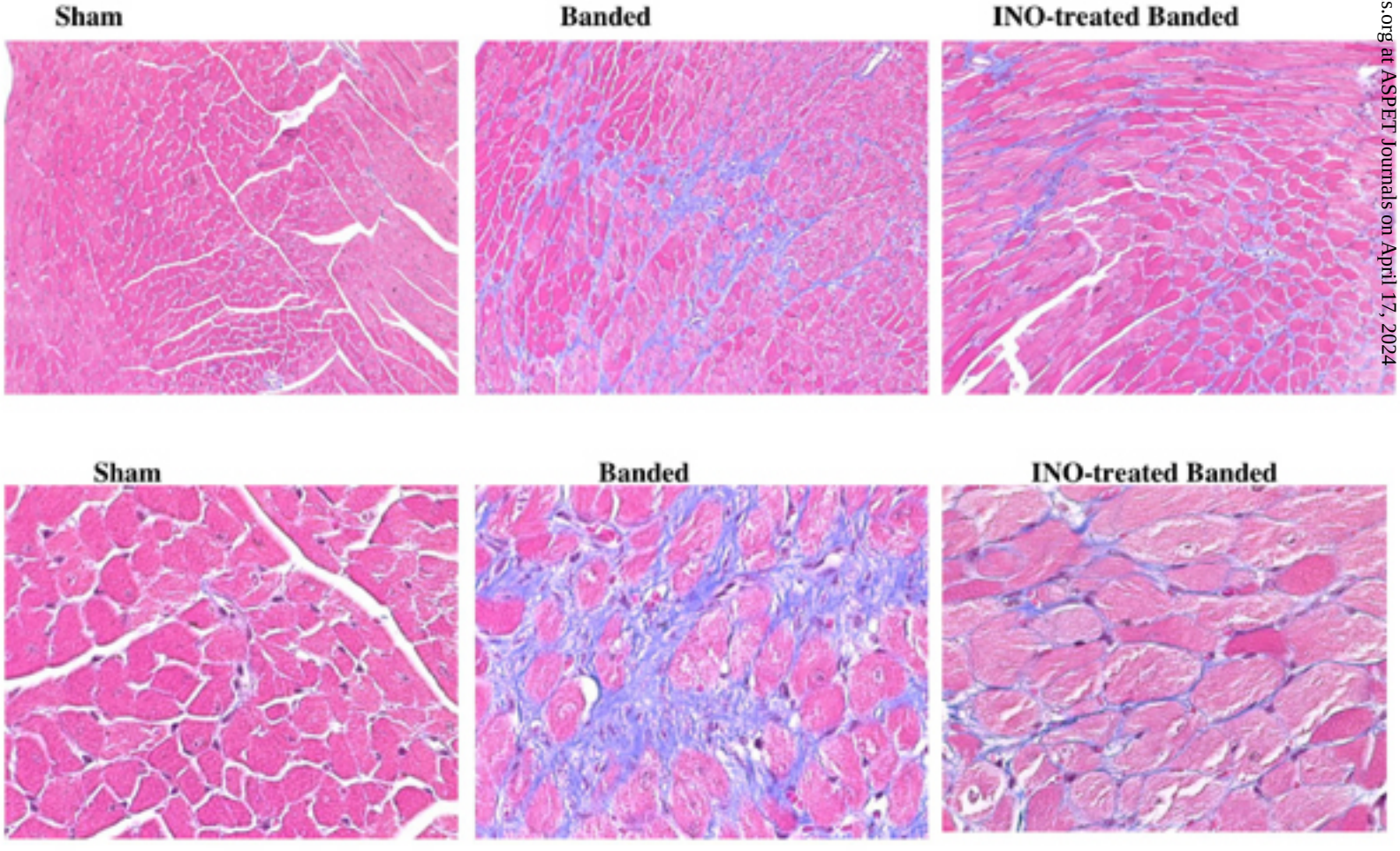

JPET Fast Forward. Published on November 2, 2004 as DOI: 10.1124/jpet.104.077164
This article has not been copyedited and formatted. The final version may differ from this version.

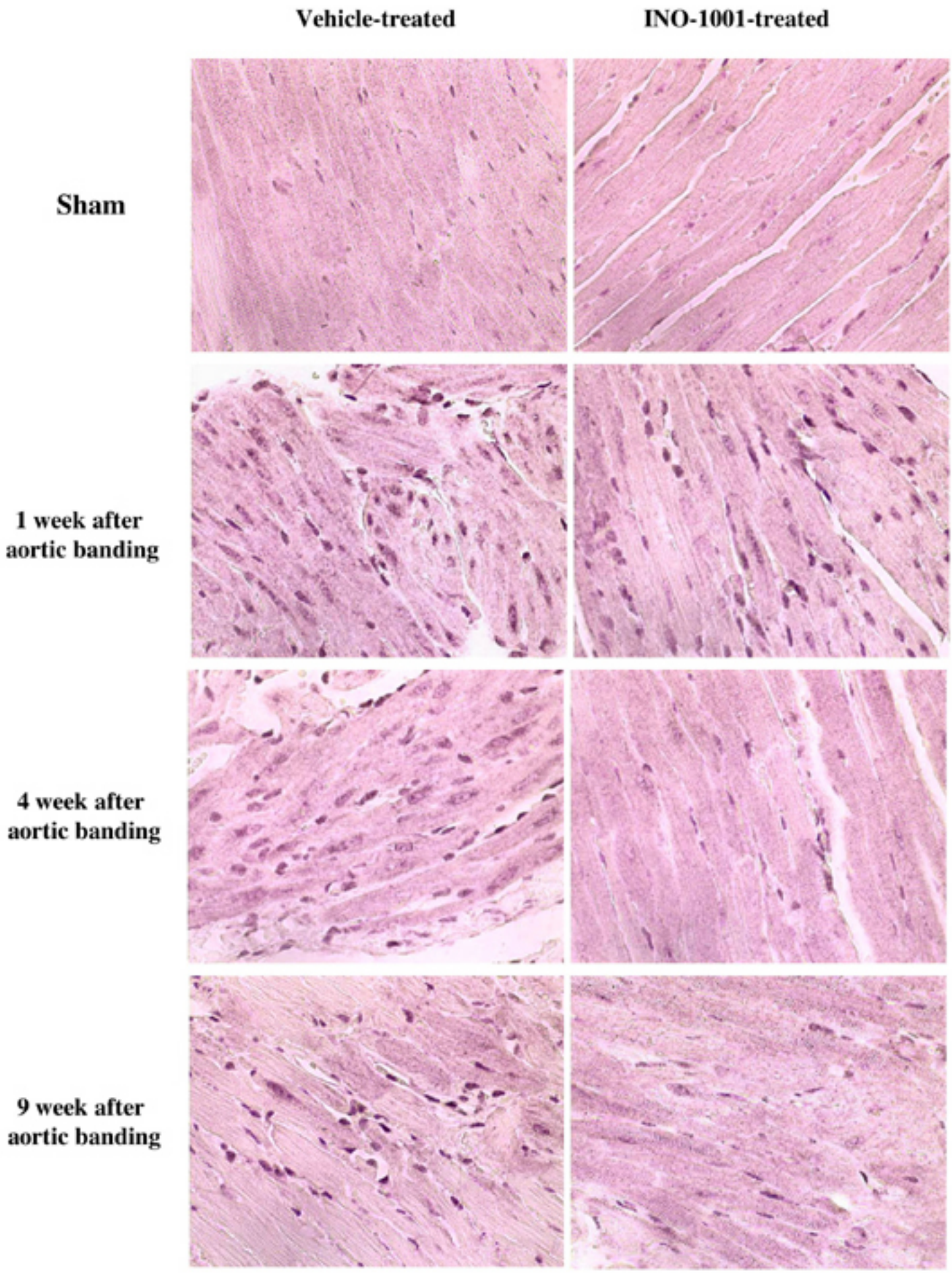

JPET Fast Forward. Published on November 2, 2004 as DOI: 10.1124/jpet.104.077164
This article has not been copyedited and formatted. The final version may differ from this version.